## Supplementary Material — Models Validation Disentangling Physical Forcings Influencing Exchange Flow in a Multi-basin Fjord System: Chiloé Inner Sea, Patagonia

Elias Pinilla and Lauren Ross
Department of Civil and Environmental Engineering
University of Maine, Orono, US.

## **Overview**

We evaluate the hydrodynamic model and forcings using three complementary diagnostics: (i) time–series overlays to assess biases, amplitude and timing; (ii) model–observation scatter to quantify linear skill (Pearson r) and typical errors (RMSE); and (iii) the global Morlet wavelet spectrum (Torrence and Compo, 1998), i.e., the time–averaged wavelet power as a function of period, which summarizes how variance is distributed across bands (semidiurnal/diurnal tides, fortnightly spring–neap, synoptic 3–12 d, and intraseasonal 25–70 d). So we pair it with time series and scatter to verify both order of magnitude agreement and banded co-variability. This is essential because our process attribution and TEF analyses rely on signals organized by those frequency bands.

To document the performance of the forcing and the hydrodynamic response, we validated (i) surface salinity against the probe on oceanographic buoy of Reloncaví Marine Observatory (OMARE) (Pérez-Santos et al., 2021) time series in Reloncaví Sound, (ii) depth-averaged axial currents at Desertores Pass against an ADCP record from oceanographic monitoring by the Fisheries Development Institute (IFOP) (Pinilla et al., 2020), (iii) along-estuary wind from the WRF-IFOP hindcast against the weather station on oceanographic buoy (OMARE), (iv) Puelo River discharge against flow gauge, and (v) sea level against the SHOA tide gauge at Puerto Montt (site map and description in Figs. S1–S6). In order: surface salinity reproduces seasonal and subtidal variability ( $r \approx 0.70$ ; Fig. S1); currents capture spring-neap modulation with skill  $(r \approx 0.93, \text{RMSE} \sim 0.11 \,\text{m s}^{-1}; \text{Fig. S2});$  the along-estuary wind compares favorably to the buoy  $(r \approx 0.84, \text{RMSE} \sim 2.3 \,\text{m s}^{-1}; \text{Fig. S3})$ ; Puelo discharge is well represented from synoptic to intraseasonal scales ( $r \approx 0.86$ , RMSE  $\sim 188 \,\mathrm{m}^3 \,\mathrm{s}^{-1}$ ; Fig. S4); and sea level matches the dominant tidal bands with high linear agreement ( $r \approx 0.97$ , RMSE  $\sim 0.40$  m; Fig. S5). Taken together, the model-forcing system matches the observed order of magnitude and exhibits coherent variance peaks across the bands that underpin our mechanism tests, indicating it is sufficiently good for the attribution and TEF diagnostics presented, within the stated limitations.

## References

- Pinilla, E., Soto, G., Soto-Riquelme, C., Venegas, O., Salas, P., and Cortes, J. (2020). Determinación de las escalas de intercambio de agua en fiordos y canales de la región de los lagos y región de aysén del general carlos ibáñez del campo. Technical report, Instituto de Fomento Pesquero (IFOP), Valparaíso, Chile.
- Pérez-Santos, I., Díaz, P. A., Silva, N., Garreaud, R., Montero, P., Henríquez-Castillo, C., Barrera, F., Linford, P., Amaya, C., Contreras, S., Aracena, C., Pinilla, E., Altamirano, R., Vallejos, L., Pavez, J., and Maulen, J. (2021). Oceanography time series reveals annual asynchrony input between oceanic and estuarine waters in patagonian fjords. *Science of The Total Environment*, 798:149241.
- Torrence, C. and Compo, G. P. (1998). A practical guide to wavelet analysis. *Bulletin of the American Meteorological society*, 79(1):61–78.

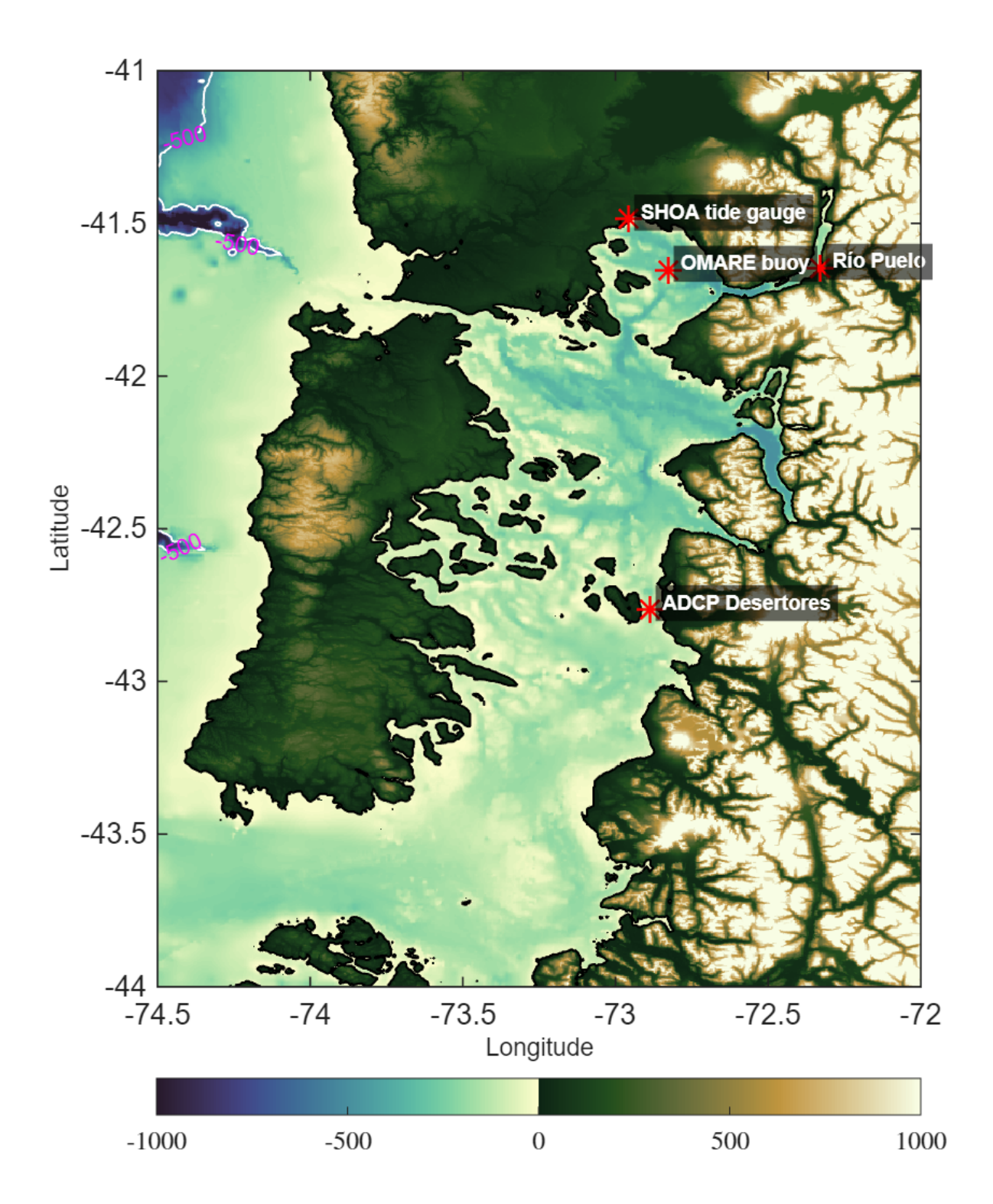


Figure S1: Validation sites in the Chiloé Inland Sea (CIS). Red asterisks mark the locations used in the supplementary figures: SHOA tide gauge at Puerto Montt (S5), OMARE buoy in Reloncaví (S1, S3), Puelo River gauging station (S4), and the ADCP mooring at Desertores Pass (S2). Background shows merged bathymetry–topography (color bar in meters; positive over land, negative at sea); magenta contours indicate isobaths on the adjacent shelf. This map provides spatial context for Figures S2–S5.

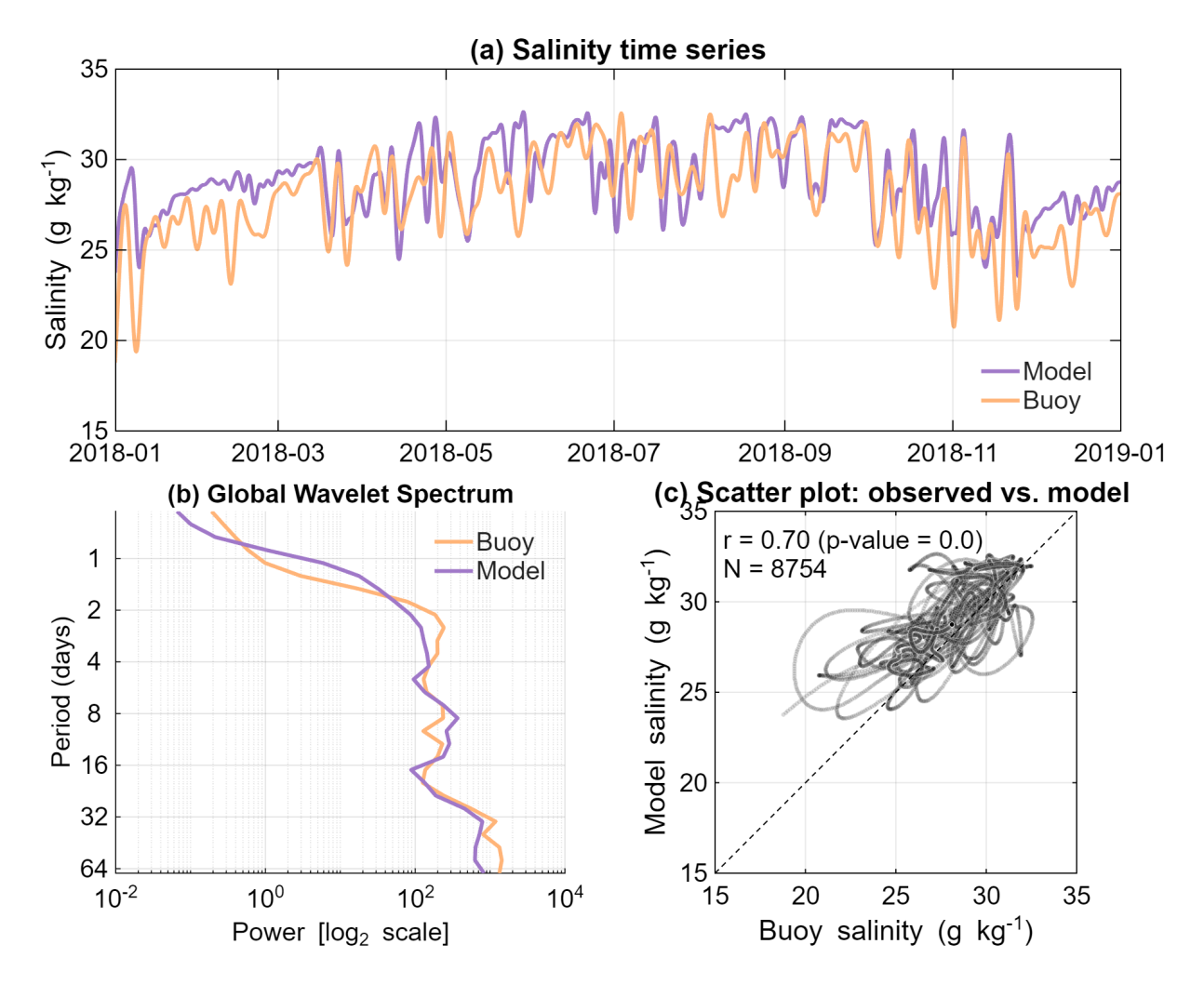


Figure S2: Validation of the hydrodynamic model's surface salinity against OMARE buoy observations (2018). The top panel (a) shows the low-pass filtered time series for the model (purple line) and buoy (orange line). The bottom left panel (b) presents the global wavelet power spectrum for buoy (orange) and model (purple), with power on a  $\log_2$  scale versus period in days. The bottom right panel (c) is a scatter plot of modeled versus observed salinity, including the Pearson correlation coefficient r=0.70 (p-value = 0.0) and number of points N=8754. All data are hourly intersected from January to December 2018 and filtered with low-pass cutoffs of 40 hours for the model and the buoy.

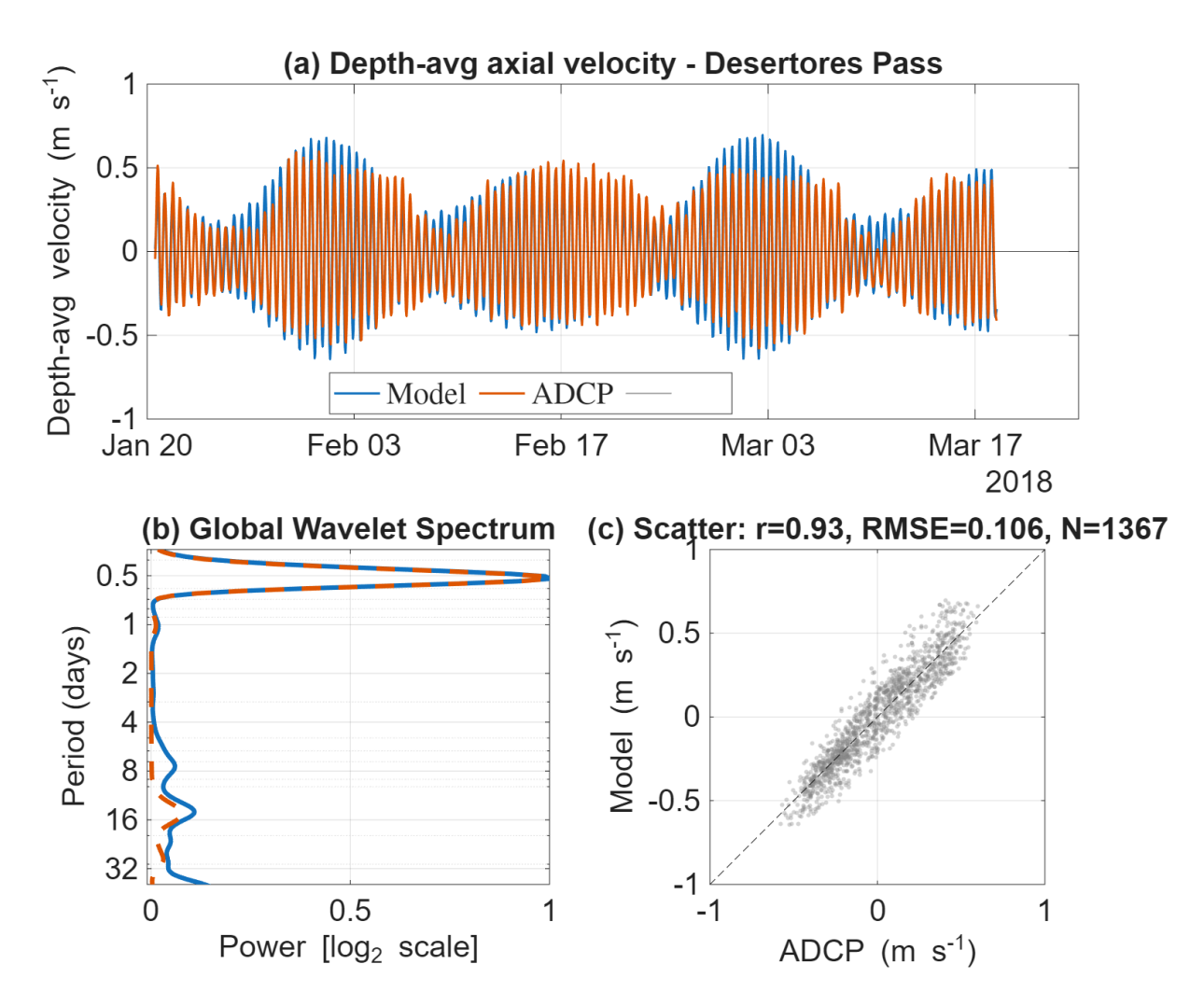


Figure S3: Validation of depth-averaged axial velocity at Desertores Pass (2018). (a) Time series of model (hourly) and ADCP (20-min data averaged to 1 h); both are depth-averaged over the instrumented water column (10–90 m), showing spring—neap modulation of the semidiurnal tide. (b) Normalized global Morlet wavelet spectrum of the depth-averaged series, with dominant energy at the semidiurnal ( $\sim$ 0.5 d) and fortnightly ( $\sim$ 15 d) bands. (c) Model–ADCP scatter with skill metrics (panel header reports r, RMSE, and N). Velocities are positive up-estuary (flood).

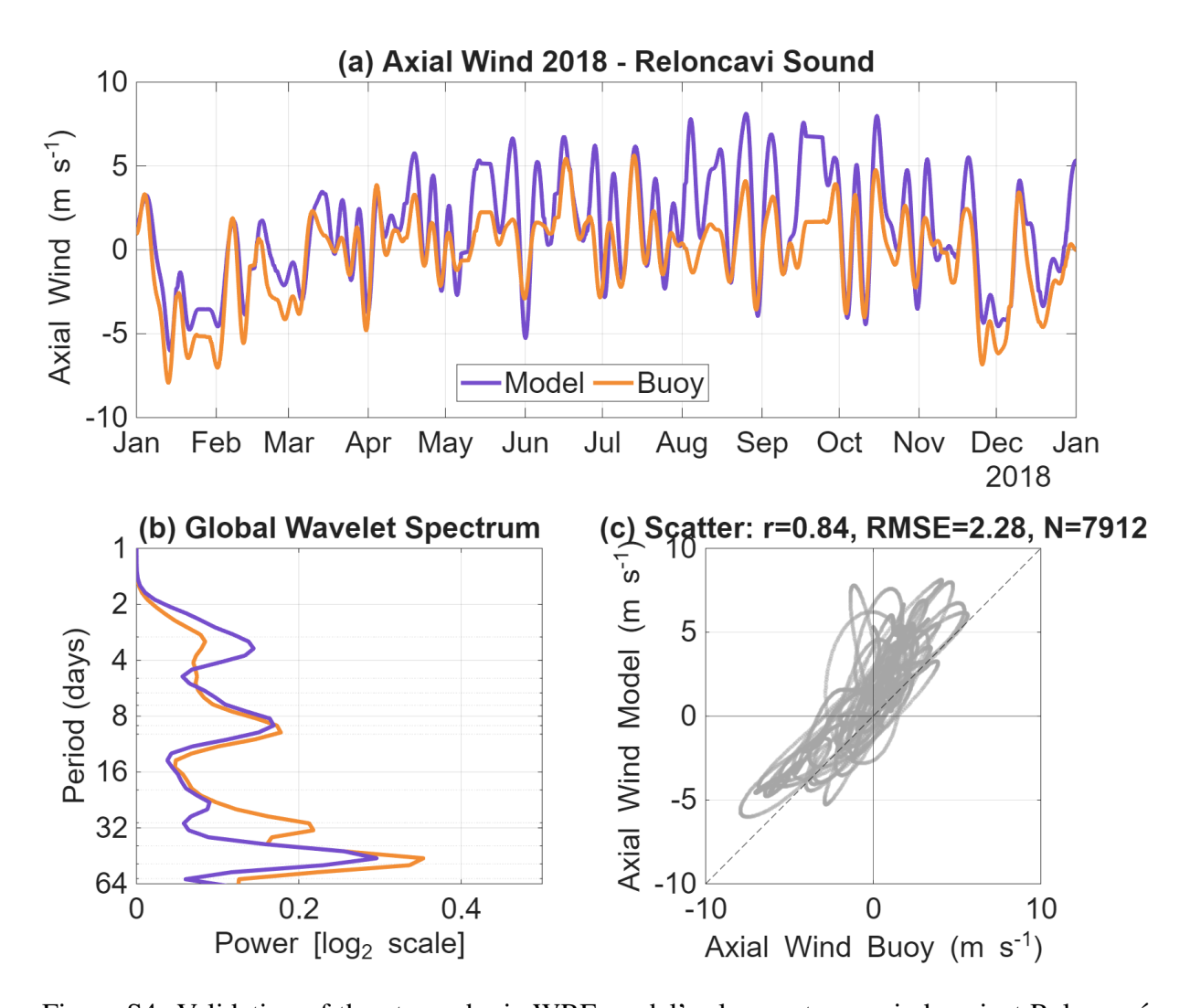


Figure S4: Validation of the atmospheric WRF model's along-estuary wind against Reloncaví Marine Observatory (OMARE) buoy observations (2018) (Pérez-Santos et al., 2021). (a) Time series for the model (purple) and buoy (orange). (b) Global wavelet power spectra (Morlet) on a  $\log_2$  power scale vs. period (days). (c) Scatter of modeled vs. observed wind with skill metrics.

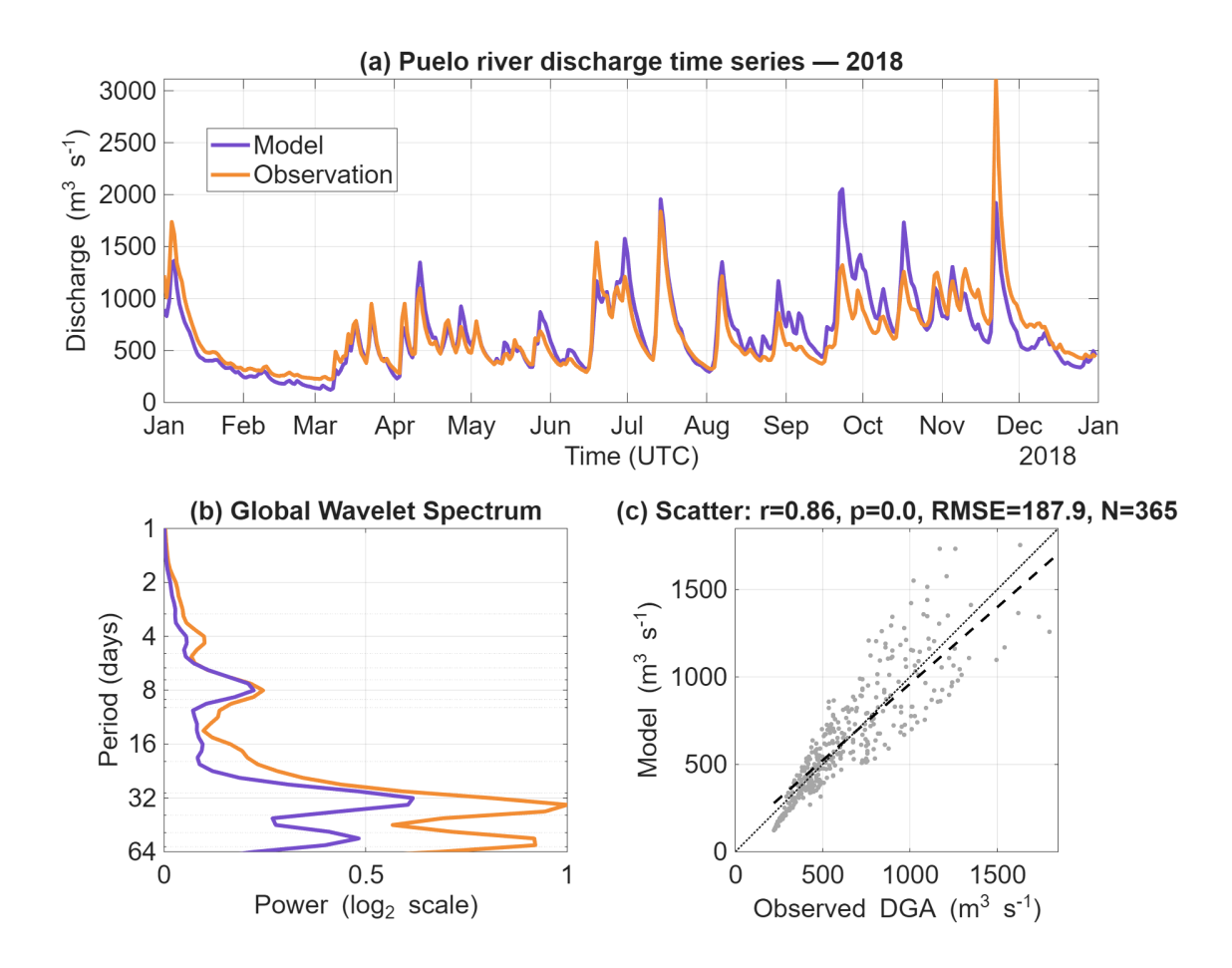


Figure S5: Validation of modeled daily discharge for the Puelo River, the main freshwater source to the Chiloé Inland Sea (CIS), for 2018. (a) Time series of discharge (m³ s $^{-1}$ ) from the National Water Agency of Chile (DGA) and from the model. (b) Normalized global Morlet spectrum with period ticks at 1, 2, 4, 8, 16, 32, and 64 days. (c) Observed vs. modeled scatter with 1:1 line and least-squares fit. Overall metrics: r = 0.86,  $p < 10^{-6}$ , RMSE = 187.9 m³ s $^{-1}$ , N = 365.

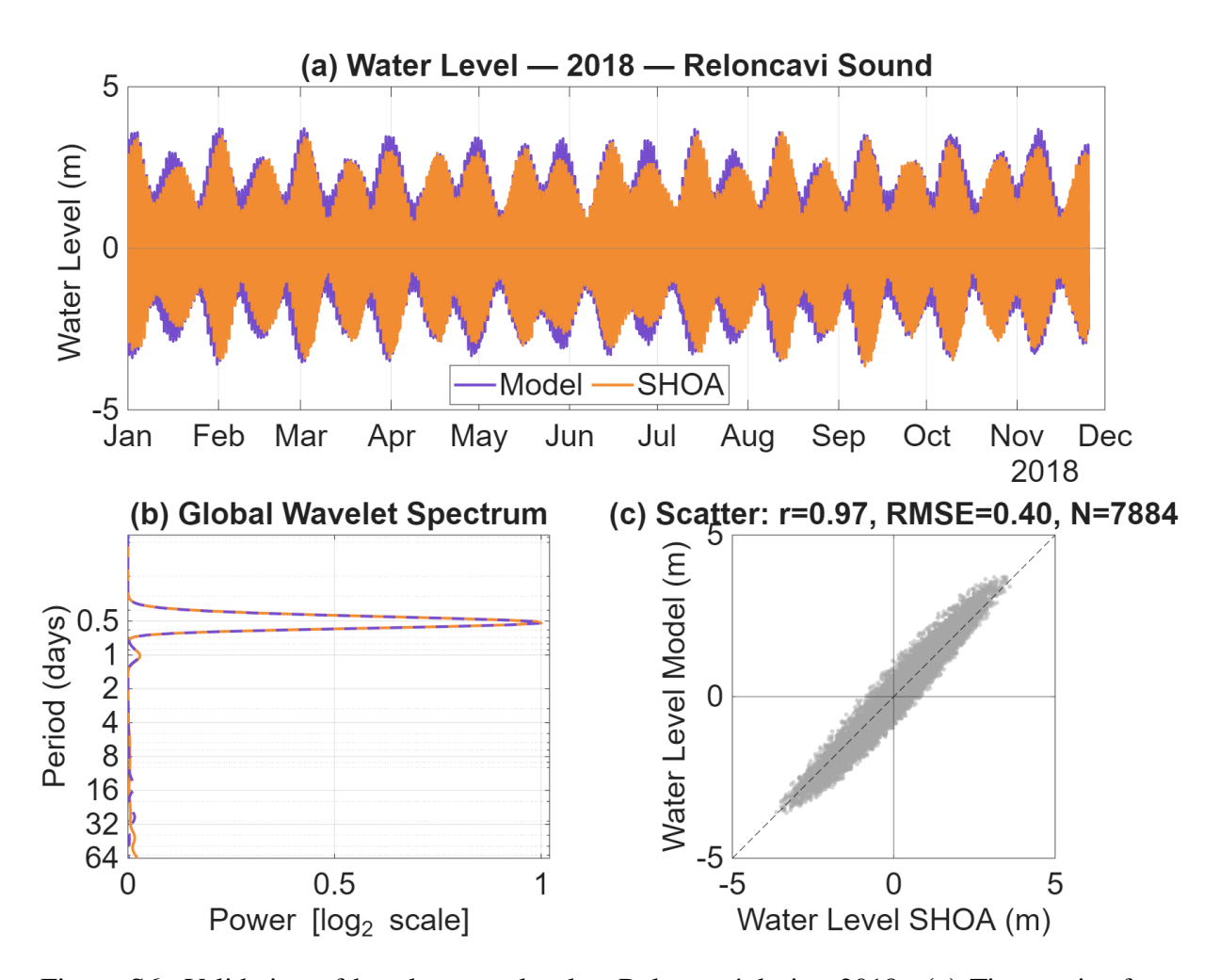


Figure S6: Validation of hourly water level at Reloncaví during 2018. (a) Time series from Hydrographic and Oceanographic Service of the Chilean Navy (SHOA) tide gauge (Puerto Montt) and model output. (b) Normalized global Morlet spectrum of the raw series; dominant energy at the semidiurnal ( $\sim$ 0.5 d) and diurnal ( $\sim$ 1 d) bands. (c) Model vs. SHOA scatter with skill metrics (reported in the panel).